Fermi National Accelerator Laboratory

FERMILAB-Pub-76/73-THY
August 1976

A Planar Bootstrap Based on a Padé Approximation to the Dual Multiperipheral Model

LOUIS A. P. BALÁZS*
Fermi National Accelerator Laboratory, Batavia, Illinois 60510
and
Physics Department, Purdue University, West Lafayette, Indiana 47907

ABSTRACT

We introduce a Padé Approximation to the multiperipheral integral equation which becomes exact for a factorizable model, but is much easier to set up, even without simplifying kinematic approximations. We then apply this to a dual multiperipheral model in which the produced clusters are dual to Regge behavior. If we only consider uncrossed loops (in the usual quark-duality sense), the requirement that the resulting output Reggeon be consistent with the input leads to two bootstrap conditions, one of which is similar to the planar bootstrap of Veneziano, but incorporates certain threshold phenomena. If we make the dual-tree approximation for the triple-Regge vertex $g(t', t'', t)$ we obtain a Reggeon intercept $\alpha_0 \simeq 0.53$ and a value for $g(0, 0, 0)$ which is in reasonably good agreement with experiment. The Pomeron can be calculated by adding in crossed (cylinder) loops and again leads to a result which is in reasonable agreement with the data at moderate energies.

---

*Supported in part by ERDA.

I. INTRODUCTION

There has recently been considerable interest in a dual-unitarization program[1, 2] for calculating strong-interaction parameters. This consists of two parts:

(i) One first does a bootstrap calculation of Reggeons using a (planar) amplitude which has exact exchange degeneracy and is unaffected by Regge-cut corrections,[3] fixed poles, diffraction and absorption.

(ii) One then makes a perturbative topological $1/N$ expansion which adds in a Pomeron and its interaction with the Reggeon and with itself.[4]

Much of the recent work on this program has been concerned with part (ii),[2, 5-8] although preliminary calculations have been made within part (i).[2, 9-12] In the present paper we will be mainly concerned with a planar bootstrap based on a dual multiperipheral model in which the produced clusters are dual to Regge behavior. We will use a Padé approximation which is exact for a factorizable model but is much easier to set up, particularly if we do not make the usual high-energy approximations. Specifically, it enables us to incorporate quite simply certain thresholds which play an important part in such models but are usually ignored in approximate treatments.[7, 8, 13]

Our equations lead to two self-consistency conditions in the forward direction. One of these is similar to the equation given by Veneziano[9] and both involve the Reggeon trajectory and triple-Reggeon coupling $g(t', t'', t)$. If we make the dual-tree approximation for g we can then calculate both the Regge intercept α_0 and $g(0, 0, 0)$.

In Sec. II we review the general multiperipheral planar bootstrap approach. In Sec. III we discuss our Padé approximation to a general multiperipheral model. This involves a single-loop graph which is discussed in Sec. IV. In Sec. V we write down our bootstrap equations and in Sec. VI we write down our results, both in a one-dimensional approximation and using our equations directly. In Sec. VII we study the effect of pion exchange, which is found to make very little difference in our results; it does lead to an Adler zero in the limit $m_\pi^2 \to 0$, however. Finally, in Sec. VIII we compare our results for the triple-Reggeon vertex with experiment.

II. THE GENERAL APPROACH

We will make the usual assumption that for meson processes, Reggeons are generated by summing the multiperipheral ladders of Fig. 1 where the vertical lines are narrow-resonance clusters a of mass $\sqrt{s_a}$. It was argued in ref. 7 that only a single meson cluster, with $s_a \simeq 0.5\ \mathrm{GeV}^2$ and corresponding to the ρ, ω, ϵ, ... peaks, is expected to be important at the sort of intermediate energies where Reggeons play any important role and where duality considerations are expected to apply. In a dual multiperipheral model the horizontal lines are linear combinations of exchange-degenerate pairs of Regge exchanges α corresponding to uncrossed (planar) quark-duality diagrams of the type shown in Fig. 2. They then correspond to Regge propagators

$$R = e^{-i\pi\alpha(t)} s^{\alpha(t)} \quad . \tag{2.1}$$

We will assume that SU(3) is exact so that the ρ - A_2, K^* - K^{**}, ω - f ϕ - f' pairs are degenerate, with

$$\alpha(t) = \alpha_0 + \alpha' t \quad . \tag{2.2}$$

All possible quark diagrams have equal weight.

In order to obtain an additional constraint on our model, we will make the assumption that the clusters a are dual in a finite-energy sum rule sense to Regge behavior. (See Fig. 3, where the external lines could be either Reggeons or particles.) This sort of constraint on sums of ladder graphs was first used a number of years ago in a pion-exchange model and has recently been applied to the dual multiperipheral model.[2, 3, 9] If Γ represents the coupling of the cluster to the external lines of Fig. 3 it leads to a relation of the form

$$\Gamma = g_1 g_2 F \quad , \tag{2.3}$$

where F is a purely kinematic factor. Although Eq. (2.3) gives a relation between Γ and $g_1 g_2$, it should be emphasized that it does not actually correspond to replacing Fig. 3(a) by 3(b), as was done in ref. 2.

The final step in the planar bootstrap is to require that the output trajectory and residue function generated by summing Fig. 1 be consistent with what goes into Fig. 1 through Eq. (2.1) and Fig. 3. We shall see

that this permits us to determine α and the triple-Regge vertex, assuming that the functional form of the latter is given by the dual-resonance model.

Once we know the parameters of the Reggeon we can calculate the Pomeron by including in the sum of Fig. 1 crossed (nonplanar) loops of the type shown in Fig. 4 in addition to the uncrossed loops of Fig. 2. In the former case we then have a Reggeon propagator

$$R = 1 s^{\alpha(t)} \quad . \tag{2.4}$$

III. A PADÉ APPROXIMATION TO THE MULTIPERIPHERAL INTEGRAL EQUATION

Let us consider $\pi\pi$ scattering. The problem of summing the multiperipheral ladders of Fig. 1 in the forward direction simplifies considerably if we take the $O(1, 3)$ partial wave of the absorptive part A

$$\tilde{A}_\lambda(m_\pi^2, m_\pi^2) = \int_{4m_\pi^2}^{\infty} ds e^{-(\lambda+1)\theta(s, m_\pi^2, m_\pi^2)} A(s) \tag{3.1}$$

where

$$e^{-\theta(s, \tau_1, \tau_2)} = 2(-\tau_1)^{\frac{1}{2}}(-\tau_2)^{\frac{1}{2}} \times \left\{(s - \tau_1 - \tau_2) + \left[(s - \tau_1 - \tau_2)^2 - 4\tau_1\tau_2\right]^{\frac{1}{2}}\right\}^{-1} \tag{3.2}$$

and A(s) is normalized so that

$$A(s) = \Delta^{\frac{1}{2}}(s, m_\pi^2, m_\pi^2)\sigma_{tot}(s) \tag{3.3}$$

with $\Delta(x, y, z) = x^2 + y^2 + z^2 - 2(xy + yz + zx)$. For our purposes m_π^2 can always be treated as negligible. If we therefore write

$$A(\lambda) = (m_\pi^2)^{\lambda+1}\tilde{A}_\lambda(m_\pi^2, m_\pi^2) \tag{3.4}$$

Eq. (3.1) reduces to

$$A(\lambda) = \int_{4m_\pi^2}^{\infty} ds\, s^{-\lambda-1} A(s) \quad , \tag{3.5}$$

which has the form of a Mellin transform.

For example, the contribution of Fig. 1(a) to A(s) is

$$V(s) = \Gamma\delta(s - s_a) \tag{3.6}$$

and so, from Eq. (3.5),

$$V(\lambda) = \Gamma s_a^{-\lambda-1} \quad . \tag{3.7}$$

The sum of Fig. 1 now has the form

$$A(\lambda) = \phi A_1(\lambda) + \phi^2 A_2(\lambda) + \ldots \tag{3.8}$$

where $\phi^i A_i$ corresponds to a ladder with i clusters; we associate a coupling-strength parameter ϕ with each cluster. In particular,

$$\phi A_1(\lambda) = V(\lambda) \tag{3.9}$$

An [N, M] Padé approximant is then defined in the usual way as the ratio[14]

$$[N, M] = \frac{\phi n_1 + \phi^2 n_2 + \ldots + \phi^N n_N}{1 + \phi d_1 + \phi^2 d_2 + \ldots + \phi^M d_M} \tag{3.10}$$

where $n_1, \ldots n_N, d_1, \ldots d_M$ are chosen so that an expansion of Eq. (3.10) in powers of ϕ agrees with the expansion (3.8) up to terms of order ϕ^{N+M}. For example

$$[1, 1] = \phi A_1(\lambda)/D(\lambda) \tag{3.11}$$

where

$$D(\lambda) = 1 - \phi A_2(\lambda)/A_1(\lambda) \ . \tag{3.12}$$

In many situations Eq. (3.10) converges more rapidly than the original sum (3.8).

In the case of a factorizable multiperipheral model it is simple to show that the [1, 1] approximation of Eq. (3.11) is in fact exact. In such a model

$$\begin{aligned} \phi A_1(\lambda) &= v(\lambda)\, v(\lambda) \\ \phi^2 A_2(\lambda) &= v(\lambda) K(\lambda)\, v(\lambda) \\ \phi^3 A_3(\lambda) &= v(\lambda) K(\lambda) K(\lambda)\, v(\lambda) \\ &\ldots\ldots\ldots\ldots\ldots \end{aligned} \tag{3.13}$$

where $v(\lambda)$ represents the external couplings and $K(\lambda)$ the internal loops of Fig. 1. (For an explicit example see Appendix A.) The series (3.8) can now be summed exactly to give

$$A(\lambda) = \frac{v^2(\lambda)}{1 - K(\lambda)} \quad . \tag{3.14}$$

But this is exactly what we would obtain from Eq. (3.11) if we take A_1 and A_2 from Eq. (3.13).

The practical advantage of using the [1, 1] Padé approximation is that we only have to evaluate the first two diagrams of Fig. 1 explicitly. If we assume that factorization is even approximately valid, as would be true with Eq. (2.3), we can evaluate the contribution of all the others by using Eq. (3.11).

IV. DUAL BOX GRAPH

We will now consider Fig. 1(b) in more detail. In the forward direction we have

$$\phi^2 A_2(s) = \frac{1}{16\pi s}\int_{t_-}^{t_+} dt\, \gamma^4_{\pi a\alpha}(t) \left|X(t)\right|^2 (\alpha' s)^{2\alpha(t)} \theta(s - 4s_a) \tag{4.1}$$

where X is the signature factor, θ is the usual step function, and

$$t_\pm \simeq -\tfrac{1}{4}\left[s^{\frac{1}{2}} \mp (s - 4s_a)^{\frac{1}{2}}\right]^2 \tag{4.2}$$

in the limit of small m_π^2.

We see that there are two kinds of threshold phenomena associated with $A_2(s)$:

(a) There is a normal threshold at $s = 4s_a$.

(b) If $\gamma^4_{\pi a\alpha}(t)$ falls off rapidly with t, A_2 is negligible below a "deferred threshold" $s \approx s_L$.[13] Suppose, for example, that $\gamma^4_{\pi a\alpha} \propto e^{Bt}$. The integrand of Eq. (4.1) is then negligible for

$$|t| \gtrsim T \equiv (B + 2\alpha' \ln \alpha' s)^{-1}$$

and so the integral itself is negligible for $|t_+| \gtrsim T$. (See Fig. 5.) The threshold s_L then comes in when $|t_+| \approx T$.

To simplify our problem further we will assume that we can replace $t_\pm$ by their asymptotic forms for $s \gtrsim s_L$. Eq. (4.1) then reduces to

$$\phi^2 A_2(s) \simeq \frac{1}{16\pi s} \int_{-\infty}^{0} dt\, \gamma^4_{\pi a\alpha}(t)\, |X(t)|^2 (\alpha' s)^{2\alpha(t)}\, \theta(s - s_L) \quad . \tag{4.3}$$

If we take the Mellin transform (3.5) of Eq. (4.3) we obtain

$$\phi^2 A_2(\lambda) \simeq \frac{s_L^{-\lambda+1}}{16\pi} \int_{-\infty}^{0} \frac{dt}{\lambda + 1 - 2\alpha(t)}\, \gamma^4_{\pi a\alpha}(t)\, |X(t)|^2 (\alpha' s_L)^{2\alpha(t)} \tag{4.4}$$

In our case it will turn out that B is not excessively large, so that s_L is not much higher than the normal threshold. We will therefore set

$$s_L \approx 4s_a \tag{4.5}$$

To relate $\gamma_{\pi a \alpha}$ to a triple-Regge coupling we will use the usual Finite-Mass Sum Rule (FMSR) for the inclusive process $\pi\pi \to \pi X$

$$\int_0^{\overline{M}_0^2} d\overline{M}^2 \frac{d\sigma}{dt\, dM^2} = \frac{G(t)}{s^2}\left(\frac{s}{\overline{M}_0^2}\right)^{2\alpha(t)}\left(\overline{M}_0^2\right)^{\alpha(0)} \tag{4.6}$$

with

$$G(t) = \frac{1}{16\pi}\gamma^2_{\pi\pi\alpha}(t)\left|X(t)\right|^2 g(t, t, 0)\gamma_{\pi\pi\alpha}(0), \tag{4.7}$$

where $\overline{M}^2 = M^2 - t - m_\pi^2$, M is the missing mass, and g is the $\alpha\alpha\alpha$ triple-Reggeon coupling. (See Fig. 6) We will assume that the low M^2 region is dominated by the production of the cluster a, so that, in the narrow-resonance approximation,

$$\frac{d\sigma}{dt\, dM^2} = \left(\frac{d\sigma}{dt}\right)_a \delta(M^2 - s_a) \ , \tag{4.8}$$

where $(d\sigma/dt)_a$ is the usual differential cross section for $\pi\pi \to \pi a$, which is given by

$$\left(\frac{d\sigma}{dt}\right)_a = \frac{1}{16\pi s^2}\gamma^2_{\pi\pi a}(t)\left|X(t)\right|^2\gamma^2_{\pi a\alpha}(t)(\alpha' s)^{2\alpha(t)} \tag{4.9}$$

The separation point M_0^2 will be taken to be midway between s_a and the next cluster above it. If we take both of these to lie on the trajectory (2.2) we then have

$$M_0^{2\alpha'} = 1.5 - \alpha_0$$

where

$$\alpha' = (1 - \alpha_0)/s_a .$$

From Eqs. (4.6) - (4.9) we now have an expression of the form (2.3)

$$\gamma^2_{\pi a\alpha}(t) = g(t, t, 0)\gamma_{\pi\pi a}(0)F_1(t) \tag{4.10}$$

where

$$\alpha' F_1(t) = \frac{\left(\overline{M}_0^{2\alpha'}\right)^{\alpha_0 + 1 - 2\alpha(t)}}{\alpha_0 + 1 - 2\alpha(t)} \quad . \tag{4.11}$$

V. BOOTSTRAP CONDITIONS

The coupling Γ in Eq. (3.6) can be related to $\gamma^2_{\pi\pi\alpha}$ by using a $\pi\pi$ finite-energy sum rule (FESR) in the forward direction

$$\int_0^N ds\ V(s) = \gamma^2_{\pi\pi\alpha}(0) N^{\alpha_0 + 1}/(\alpha_0 + 1) \quad , \tag{5.1}$$

where N is a point between the ρ and f resonances. From Eqs. (3.6) and (5.1) we then have

$$\Gamma = \gamma^2_{\pi\pi\alpha}(0) F_0 \quad , \tag{5.2}$$

with

$$F_0 = N^{\alpha_0 + 1}/(\alpha_0 + 1) \quad . \tag{5.3}$$

To avoid having to pick a specific value for N we could follow the alternative procedure of using the $\pi\pi$ Lovelace-Veneziano model. This has both duality and crossing built in and is approximately consistent with experiment. It gives a relation (5.2) with

$$\alpha' F_0 = \Gamma\big(\alpha(t) + 1\big) \quad . \tag{5.4}$$

This is the form we will use from now on.

From Eqs. (3.11), (3.12), (3.9), (3.7), (4.4), (4.10) and (5.2), we now have

$$A(\lambda) = V(\lambda)/D(\lambda) \tag{5.5}$$

with

$$V(\lambda) = \gamma^2_{\pi\pi\alpha}(0) F_0 s_a^{-\lambda - 1} \quad , \tag{5.6}$$

$$D(\lambda) = 1 - \frac{1}{16\pi F_0}\left(\frac{s_a}{s_L}\right)^{\lambda+1} \int_{-\infty}^{0} dt \, \frac{H(t)}{\lambda + 1 - 2\alpha(t)} \quad , \tag{5.7}$$

and

$$H(t) = g^2(t, t, 0)\,|X(t)|^2\, F_1^{\,2}(t)(\alpha' s_L)^{2\alpha(t)} \quad . \tag{5.8}$$

Eq. (5.5) has an output pole at $\lambda = \alpha$ if

$$D(\alpha) = 0 \quad . \tag{5.9}$$

The corresponding residue is then

$$\gamma^2_{\pi\pi\alpha}(0) = V(\alpha)/D'(\alpha) \quad . \tag{5.10}$$

We will require that this output pole be consistent with the input. From Eqs. (5.9) and (5.6) we then have

$$D'(\alpha) = F_0 s_a^{-\alpha - 1} \quad . \tag{5.11}$$

Note that the conditions (5.9) and (5.10) are both independent of $\gamma_{\pi\pi\alpha}$ and are essentially constraints on α and g.

To have a complete bootstrap we have to know the t dependence of g(t, t, 0). We will assume a dual-tree model of the Neveu-Schwartz type, which has no tachyon on the ρ - f trajectory. This gives[3, 10, 12]

$$g^2(t, t, 0)\,|X(t)|^2 = N\bar{g}^2\Gamma(\alpha_0)\frac{\Gamma^2(1 - \alpha(t))}{\Gamma^2(\alpha_0 + 1 - 2\alpha(t))} \tag{5.12}$$

where N is the number of quarks. Since we are assuming SU(3) we have N = 3. The above equations are now sufficient to determine all the parameters in our model.

V. RESULTS

Eq. (5.7) involves a non-elementary integral. The integrand falls off fairly rapidly with t, however, and so we will approximate H by an exponential

$$H(t) \simeq H_0 e^{2ct} \tag{6.1}$$

with H_0 and c adjusted so that the approximation is exact at $t = 0$ and $t = -\frac{1}{2}(\alpha_0/\alpha')$. The results are not sensitive to this prescription. They are not very different, for example, if we adjust H_0 and c so that the value and derivative are exact at $t = 0$.

A. The One-Dimensional Approximation

Before proceeding to a more exact treatment we will make the rather crude approximation that the rapid falloff of H(t) permits us to replace the denominator in the integral of Eq. (5.7) by its value at $t = 0$. We then have

$$D(\lambda) = 1 - \left(\frac{s_a}{s_L}\right)^{\lambda+1} \frac{k}{\lambda + 1 - 2\alpha_0} \tag{6.2}$$

with

$$k = \frac{1}{16\pi F_0} \int_{-\infty}^{0} H(t)\, dt \quad . \tag{6.3}$$

If we now impose the conditions (5.9) and (5.11) and use Eqs. (6.1), (5.8), (5.12), (5.3), (4.11) and (4.5), we obtain

$$\alpha_0 = 0.60 \quad , \quad N\bar{g}^2/16\pi = 0.53 \quad . \tag{6.4}$$

These values are close to those obtained by Schaap and Veneziano,[10] although we shall see that the g is somewhat smaller than is indicated by experiment. It should be emphasized that our calculation gives a specific value for α_0, rather than just a range, as in ref. 10.

B. The Reggeon Parameters

If we do not use the one-dimensional approximation, Eqs. (5.7) and (6.1) give

$$D(\lambda) = 1 - \frac{H_0}{32\pi\alpha' F_0} e^{-2c\alpha_0/\alpha'} \left(\frac{s_a}{s_L} e^{c/\alpha'} \right)^{\lambda+1} E_1\left(\frac{c}{\alpha'} (\lambda + 1 - 2\alpha_0) \right) \tag{6.5}$$

where E_1 is the usual exponential integral. Imposing, as before, the conditions (5.9) and (5.11), we obtain

$$\alpha_0 = 0.53 \quad , \quad N\bar{g}^2/16\pi = 1.36 \quad . \tag{6.6}$$

These are closer to the experimental values.

C. The Pomeron Parameters

As discussed in Sec. II, the Pomeron can be calculated by adding in the cylinder loops of Fig. 2. In the forward direction the only effect is to make the replacements

$$A_2(\lambda) \to 2A_2(\lambda) \tag{6.7}$$

or

$$H(t) \to 2H(t) \tag{6.8}$$

in the vacuum state, since $|1|^2 = |e^{-i\pi\alpha(t)}|^2$. If we again use Eqs. (5.9) and (5.10) but with $\alpha \to \alpha_P$ we obtain

$$\alpha_P = 0.80, \quad \gamma^2_{\pi\pi P} = 1.45\, \gamma^2_{\pi\pi f} . \tag{6.9}$$

This is similar to the results obtained in ref. 7. The f itself becomes extinct in such a calculation. Our "Pomeron," of course, is only an effective pole which describes the cross section at intermediate energies.[15, 1] To obtain the (bare) Pomeron which describes scattering at higher energies we would have to include higher-mass clusters, as discussed in ref. 7.

VII. PION EXCHANGE

In the above calculation we have made the assumption that the dominant exchanges α come from the leading (vector-tensor) Reggeon trajectories. Because of the small mass of the pion, however, we might expect its contribution to be nonnegligible. To estimate it we will continue to use the [1, 1] Padé approximation of Eq. (3.11) but include pion exchange in Fig. 1(b) when we evaluate $\phi^2 A_2(\lambda)$. In the vacuum state the only change is to make the replacement

$$A_2 \to A_2^{R+\pi} = A_2 + A_2^{\pi} \tag{7.1}$$

with A_2^{π} given by Fig. 7, which gives

$$\phi^2 A_2^{\pi} = \frac{1}{16\pi^3 s} \int_{t_-}^{t_+} dt \left(\frac{\Gamma}{m_\pi^2 - t} \right)^2 Q(t)\theta(s - 4s_a) \ , \tag{7.2}$$

where $Q(t)$ is an off-shell factor. We will take $\Gamma \simeq 50$, which corresponds to a ρ width of 0.15 GeV if we assume that Eq. (3.6) is given by the Lovelace-Veneziano model.

For simplicity we will assume an elementary pion and make two different assumptions for Q.

(i) With $Q = 1$, Eqs. (7.2), (4.2) and (3.5) give

$$\phi^2 A_2^{\pi}(\lambda) = \frac{\Gamma^2}{32\pi^3} \frac{\Gamma^2(\lambda)}{\Gamma(2\lambda)} \frac{s_a^{-\lambda - 2}}{2\lambda + 1} \tag{7.3}$$

The conditions (5.9) and (5.11) now give

$$\alpha_0 = 0.54 \quad , \quad N\bar{g}^2/16\pi = 1.13 \ . \tag{7.4}$$

(ii) With the rather strong off-shell factor[17]

$$Q(t) \simeq (1 - t/s_a)^2 \tag{7.5}$$

Eqs. (7.2), (4.2) and (3.5) give

$$\phi^2 A_2^{\pi}(\lambda) = \frac{\Gamma^2}{16\pi^3} \frac{\Gamma^2(\lambda)}{\Gamma(2\lambda)} \frac{s_a^{-\lambda - 2}}{\lambda + 1} \ . \tag{7.6}$$

The conditions (5.9) and (5.11) now give

$$\alpha_0 = 0.54, \quad N\bar{g}^2/16\pi = 0.82. \tag{7.7}$$

The factor (7.5) probably exaggerates the large $|t|$ behavior, however.

We conclude that pion exchange has very little effect on α_0 and does not significantly lower g^2, especially with $Q = 1$.

Adler Zero: Although pion exchange does not affect our planar bootstrap in any important way it should perhaps be mentioned in passing that it can be dominant for certain effects. For example we see from Eq. (7.3) that $A_2^{\pi}(\lambda) \to \infty$ as $\lambda \to 0$. From Eqs. (3.12) and (3.11) this in turn means that $A(\lambda = 0) = 0$. But from Eq. (3.5)

$$\frac{1}{\pi} A(\lambda = 0) = \frac{1}{\pi} \int_{4m_\pi^2}^{\infty} ds \, \frac{A(s)}{s} = \frac{1}{2} T(s = 0) \tag{7.8}$$

where $T(s)$ is the forward $\pi\pi$ amplitude and where we have used the fact that it satisfies a dispersion relation. But then

$$T(s = 0) = 0,$$

which is just the Adler zero in the limit of zero pion mass.

VIII. COMPARISON WITH EXPERIMENT

Our calculated α_0 is very close to the experimental value. In principle, g can be extracted from an inclusive process $a + b \to c + X$ in the triple-Regge region, where the cross section is related to the absorptive part of Fig. 8. In practice, however, it is difficult to isolate the desired vertex. We will consider three different processes.

A. Chan et al.[2] isolated the g vertex in $K^- p \to X^- p$ by summing only over resonances in X^-, using semi-local duality, so $i = j = k = f - \omega$. For $s = 20\ \text{GeV}^2$, $M^2 = 2.15\ \text{GeV}^2$, $t = -0.1\ \text{GeV}^2$, this gives

$$d\sigma/dt\, dM^2 = 0.30 \pm 0.06\ \text{mb/GeV}^4 . \tag{8.1}$$

In terms of our notation, the same cross section is given by

$$\frac{d\sigma}{dt\, dM^2} = \frac{\tilde{G}_{ijk}(t)}{s^2}\left(\frac{s}{\overline{M}^2}\right)^{\alpha_i(t) + \alpha_j(t)} (\overline{M}^2)^{\alpha(0)} \tag{8.2}$$

where

$$\tilde{G}_{\alpha\alpha\alpha} = \frac{1}{\sqrt{2}}\, \gamma^2_{pp\alpha}\, \overline{g}\, \gamma_{KK\alpha} \sin \pi\alpha \tag{8.3}$$

if we approximate $\tilde{G}$ by its value at $t = 0$. Now the experimental $\frac{1}{2}(\sigma_{\bar{p}p} - \sigma_{pp})$, which is dominated by ω exchange, gives $\gamma^2_{pp\omega} = \gamma^2_{pp\alpha} \simeq 83.8$ (in GeV units). The quark model gives $\gamma_{KK\alpha} = \frac{1}{2}\gamma_{\pi\pi\alpha}$ and $\gamma_{\pi\pi\alpha} = \frac{2}{3}\gamma_{pp\alpha}$. If we use our result (7.4) we then obtain

$$d\sigma/dt\, dM^2 \simeq 0.30 \text{ mb/GeV}^4 , \tag{8.4}$$

which agrees quite well with Eq. (8.1).

B. Dash analyzed the process $pp \to pX$ in terms of a "Pomeron" P with $\alpha_P = 0.85$, which is similar to the one obtained in Eq. (6.9).[15] He assumed that it was dominated by Fig. 8 with ijk = $\pi\pi P$ and PPP and obtained

$$\tilde{G}_{PPP}(0) \simeq 2000 \text{ (GeV units)} . \tag{8.5}$$

We can calculate $\tilde{G}_{PPP}$ in terms of $\bar{g}$ by using the result (6.9) and assuming the sort of generalized f/P universality[18] discussed in ref. 7, which gave a coupling ratio

$$\gamma_{xyP}/\gamma_{xyf} = (s_R/s_a)^{\alpha - \alpha_P} \gamma_{\pi\pi P}/\gamma_{\pi\pi f} , \tag{8.6}$$

where $\sqrt{s_R}$ is the mass of the end cluster in the particular multiperipheral ladder sum which gives rise to our Regge couplings, and x and y could be either particles or Reggeons. If we apply Eq. (8.6) to all the vertices of Fig. 8,[19] using the fact that the end clusters are nucleons in the case of the proton vertices and particles with mass $\simeq m_\rho$ at the triple-Regge vertex, we obtain from Eqs. (8.3) and (7.4)

$$\tilde{G}_{PPP}(0) = 2691 \text{ (GeV units)} . \tag{8.7}$$

This is slightly larger than the value in Eq. (8.5), but we must remember that our calculated α_P is smaller than the one assumed by Dash.[15]

C. In the case of $K^- p \to \overline{K^0} X$ we have $i = j = \rho - A_2$ and $k = P$. If we again apply our generalized f/P universality (8.6) to the vertices involving P we can calculate the coupling $\tilde{G}_{ijk}$. If we approximate this by its value at $t = 0$ we obtain

$$d\sigma/dt\, dM^2 = 0.21 \text{ mb/GeV}^4 \tag{8.8}$$

for $s = 16 \text{ GeV}^2$, $M^2 = 2.8$ and $t = -0.1 \text{ GeV}^2$. The corresponding experimental value is

$$d\sigma/dt\, dM^2 = 0.33 \text{ mb/GeV}^4 \quad . \tag{8.9}$$

A possible explanation for the above discrepancy is the fact that we have only included the multiperipheral component (P_M) and have neglected the diffractive part of the Pomeron (P_D). The latter was found to be quantitatively important in ref. 7 for pp scattering, even though it can be argued to be less important for the PPP coupling considered in (B).[20] We can estimate its contribution by using the fact that f/P universality applies separately to P_M and P_D.[20] This in turn means that the P_D/P_M coupling ratio r should itself be approximately universal, i.e., independent of the process involved. In ref. 7 it was found to be $r = L/\gamma^2_{PP\hat{P}} \simeq 62.9/110$ for pp scattering. We must therefore multiply Eq. (8.8) by $(1 + r)$ if

we wish to include P_D as well as P_M. We then obtain

$$d\sigma/dt\, dM^2 \simeq 0.33 \text{ mb. GeV}^4 \quad . \tag{8.10}$$

IX. CONCLUSION

We have used a Padé approximation to a dual multiperipheral model and the dual-tree approximation for the triple-Reggeon vertex g. We then

(a) Made a self-consistent calculation of α_0 and g^2, which are in reasonable agreement with experiment.

(b) Calculated reasonable values for the trajectory intercept and residue function of the effective Pomeron which describes scattering and inclusive processes at intermediate energies.

(c) Included the effect of pion exchange and found that it does not change the planar bootstrap of α_0 and g^2 in any substantial way.

Further calculations might involve

(i) Evaluating the integrals (4.1) and (3.5) more accurately. A direct inverse Mellin transform of Eq. (3.11) might then be expected to give a detailed picture of the behavior of the cross section both in the case of the Reggeon, and in the case of the Pomeron if we make the replacement (6.7).

(ii) Going away from the forward direction. This may tell us something about the t dependence of g and $\alpha(t)$. It may be possible to obtain another

constraint on our equations by taking advantage of the fact that a parameter like α' is needed to fix the energy scale of the problem.

ACKNOWLEDGMENTS

The author would like to thank Prof. B. W. Lee and Prof. C. Quigg for their hospitality at the Fermi National Accelerator Laboratory, where part of this work was done.

APPENDIX. EXAMPLE OF A FACTORIZABLE MODEL

We will illustrate Eq. (3.13) by considering a simple approximation to the Amati-Bertocchi-Fubini-Stanghellini-Tonin equation.[21] In the forward direction this has the form[22]

$$\tilde{A}_\lambda(\tau_1, \tau_2) = \tilde{V}_\lambda(\tau_1, \tau_2) + \frac{1}{16\pi^3(\lambda+1)} \int_{-\infty}^{0} \frac{d\tau'}{(m_\pi^2 - \tau')^2} \tilde{V}_\lambda(\tau_1, \tau_2)\tilde{A}_\lambda(\tau_1, \tau_2) \quad \text{(A.}$$

where $\tilde{A}_\lambda$ and $\tilde{V}_\lambda$ are off-shell versions of the projection (3.1) of A and V. Our approximation is to replace Eq. (3.2) by[23]

$$e^{-\theta(s, \tau_1, \tau_2)} \simeq s(-\tau_1)^{\frac{1}{2}}(-\tau_2)^{\frac{1}{2}}(s - \tau_1)^{-1}(s - \tau_2)^{-1} \tag{A.2}$$

From Eq. (3.6) we then have

$$\tilde{V}_\lambda(\tau_1, \tau_2) = w_\lambda(\tau_1) w_\lambda(\tau_2) \tag{A.3}$$

where

$$w_\lambda(\tau) = \Gamma^{\frac{1}{2}}\left[s_a(-\tau)^{\frac{1}{2}}/(s_a - \tau)\right]^{\lambda+1} \tag{A.4}$$

Explicit calculations have shown that the resulting solution of Eq. (A.1) is good to within about 10% for relevant values of the input parameters.[23]

If we now iterate Eq. (A.1), using Eq. (A.3), we have

$$\tilde{A}_\lambda(\tau_1, \tau_2) = w_\lambda(\tau_1)w_\lambda(\tau_2) + w_\lambda(\tau_1)K(\lambda)w_\lambda(\tau_2) + w_\lambda(\tau_1)K(\lambda)K(\lambda)w_\lambda(\tau_2) + \ldots \tag{A.5}$$

where

$$K(\lambda) = \frac{1}{16\pi^3(\lambda+1)} \int_{-\infty}^{0} \frac{d\tau}{\left(m_\pi^2 - \tau\right)^2} \; w_\lambda^2(\tau) \quad . \tag{A.6}$$

If we then use Eq. (3.4) we see that Eq. (A.5) reduces to the series (3.8), where the terms are given by Eq. (3.13) with

$$v(\lambda) = m_\pi^{\lambda+1} w_\lambda(m_\pi^2) \quad . \tag{A.7}$$

REFERENCES

[1] G. Veneziano, Nucl. Phys. B74, 365 (1974); Phys. Lett. 52B, 220 (1974).

[2] Chan Hong-Mo, J. E. Paton and Tsou Sheung Tsun, Nucl. Phys. B86, 479 (1975); Chan Hong-Mo, J. E. Paton, Tsou Sheung Tsun and Ng Sing Wai, Nucl. Phys. B92, 13 (1975).

[3] M. Bishari and G. Veneziano, Phys. Lett. 58B, 445 (1975).

[4] Huan Lee, Phys. Rev. Lett. 30, 719 (1973); G. Veneziano, Phys. Lett. 43B, 413 (1973); Chan Hong-Mo and J. E. Paton, Phys. Lett. 46B, 228 (1973).

[5] C. Rosenzweig and G. F. Chew, Phys. Lett. 58B, 93 (1975); Nucl. Phys. B104, 290 (1976).

[6] C. Schmid and C. Sorensen, Nucl. Phys. B96, 209 (1975); N. Papadopoulos, C. Schmid, C. Sorensen and D. M. Webber, Nucl. Phys. B101, 189 (1975); C. B. Chiu, M. Hossain and D. M. Tow, Univ. of Texas report ORD251 (1976); N. Sakai, Nucl. Phys. B99, 167 (1975).

[7] L. A. P. Balázs, Vacuum Singularities in a Dual Multiperipheral Model, FERMILAB-Pub-76/56-THY (1976); Phys. Lett. 61B, 187 (1976).

[8] J. Dash, Phys. Lett. 61B, 199 (1976); J. Dash and S. T. Jones, Rising Cross Sections and the Flavoring of the Pomeron, Lawrence Berkeley Laboratory Report LBL-5337 (1976).

[9] C. Rosenzweig and G. Veneziano, Phys. Lett. 52B, 335 (1974).

[10] M. M. Schaap and G. Veneziano, Lett. Nuovo Cim. 12, 204 (1975).

[11] J. Kwiecinski and N. Sakai, Nucl. Phys. B106, 44 (1967).

[12] Ken-ichi Konishi, Symmetry Breaking and Planar Bootstrap Equations, Rutherford Laboratory Report RL-76-036, T. 157 (1976).

[13] G. F. Chew and D. Snider, Phys. Lett. 31B, 75 (1970); G. F. Chew and J. Koplik, Phys. Lett. 48B, 221 (1974).

[14] G. A. Baker, Jr., Essentials of Padé Approximants, Academic Press, N.Y. (1975).

[15] J. Dash, Phys. Rev. D9, 200 (1974).

[16] N. Bali and J. Dash, Phys. Rev. D10, 2102 (1974).

[17] J. Dash, G. Parry and M. Grisaru, Nucl. Phys. B53, 91 (1973).

[18] R. Carlitz, M. B. Green and A. Zee, Phys. Rev. D4, 3439 (1971).

[19] L. A. P. Balázs, Phys. Rev. D11, 1071 (1975).

[20] L. A. P. Balázs and P. D. Rittman, Phys. Rev. D13, 3130 (1976).

[21] D. Amati, A. Stanghellini and S. Fubini, Nuovo Cimento 26, 896 (1962); L. Bertocchi, S. Fubini and M. Tonin, ibid. 25, 626 (1962).

[22] S. Nussinov and J. Rosner, J. Math. Phys. 7, 1670 (1966).

[23] Chun-Fai Chan and B. R. Webber, Phys. Rev. D5, 933 (1972).

FIGURE CAPTIONS

Fig. 1: The absorptive part for a multiperipheral cluster model.

Fig. 2: Uncrossed (planar) quark-duality diagram.

Fig. 3: Average duality relation between cluster (a) and Reggeon (b).

Fig. 4: Nonplanar (cylinder) quark-duality diagram with crossed and uncrossed loops.

Fig. 5: Integration range in the integral of Eq. (4.1).

Fig. 6: Finite-mass sum rule for $\pi\pi \to \pi X$ relating the cluster-production and triple-Regge regions.

Fig. 7: Box graph with pion exchange.

Fig. 8: A triple-Regge graph which contributes to the cross section for $a + b \to c + X$ in the triple-Regge region.

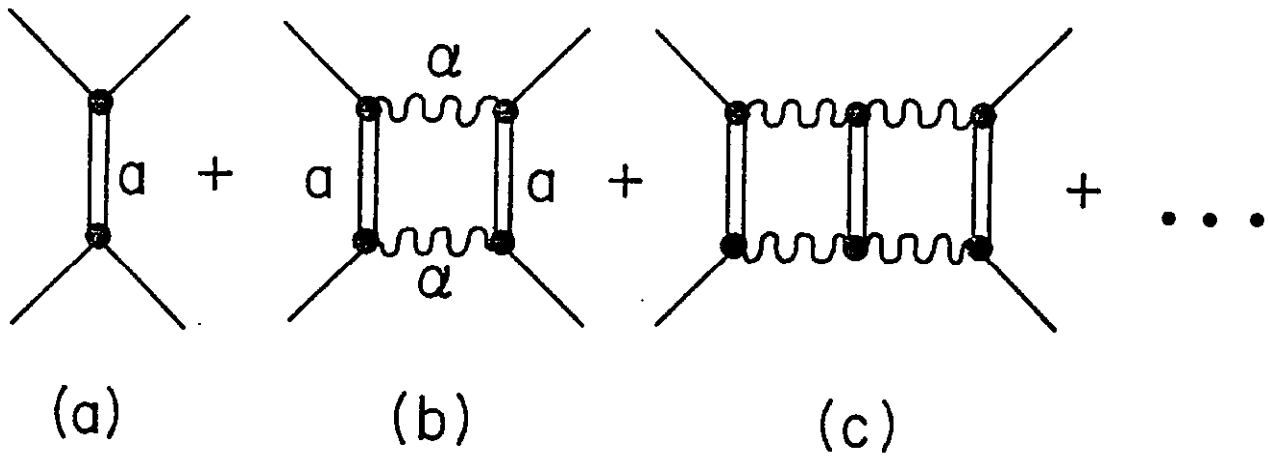

Fig. 1

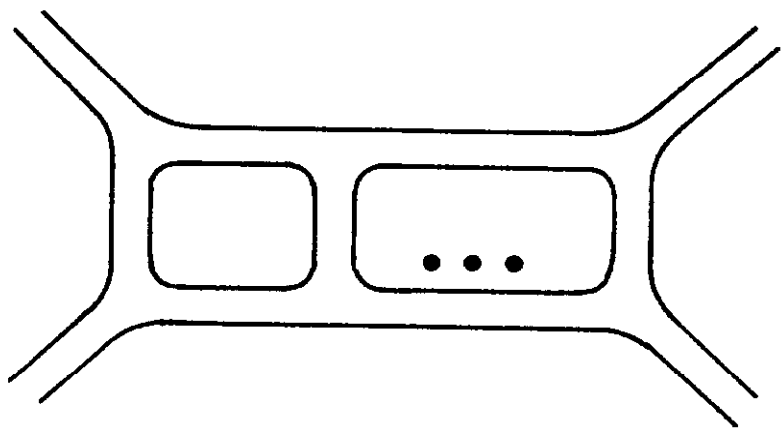

Fig. 2

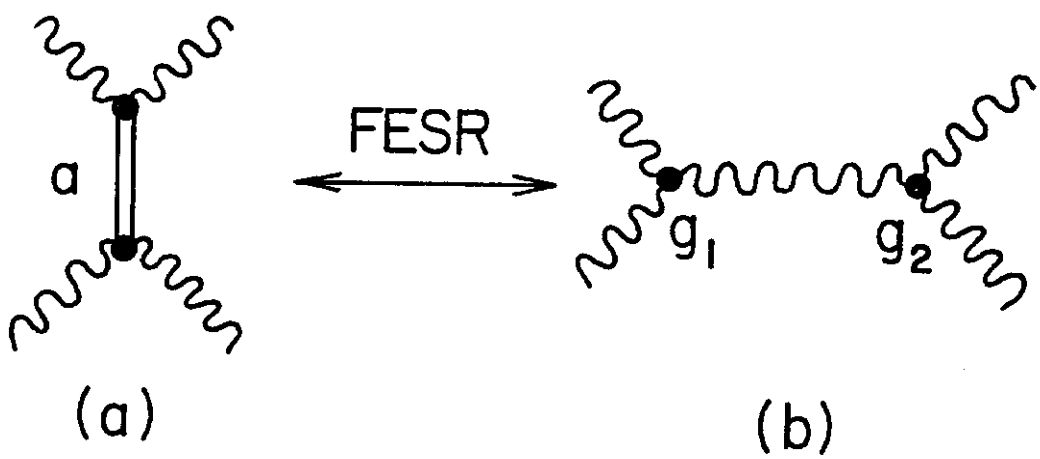

Fig. 3

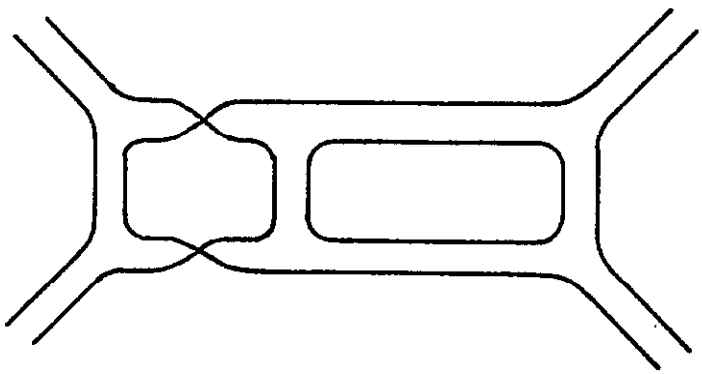

Fig. 4

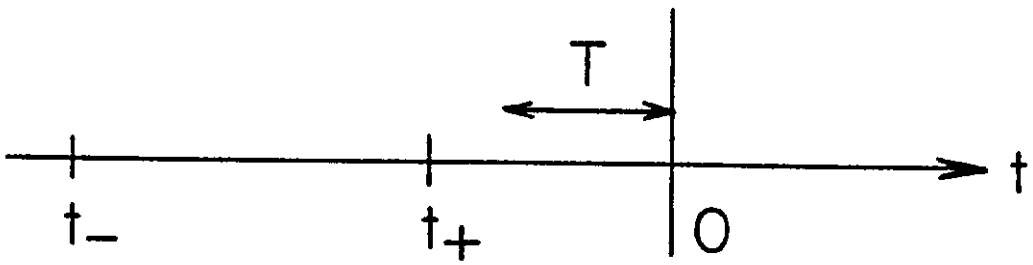

Fig. 5

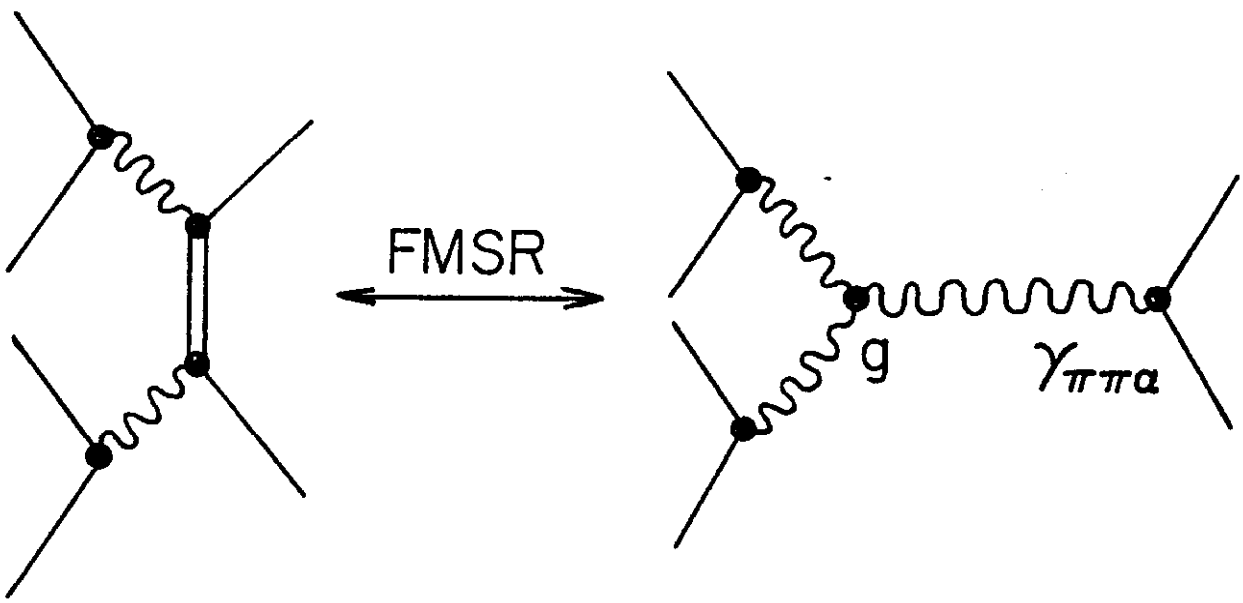

Fig. 6

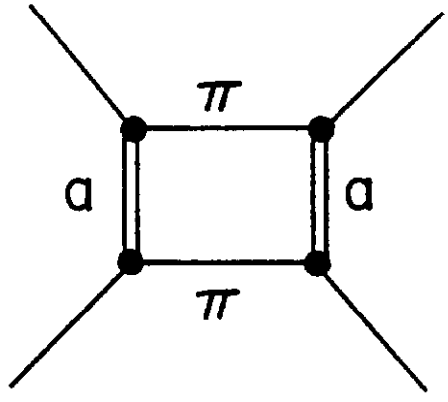

Fig. 7

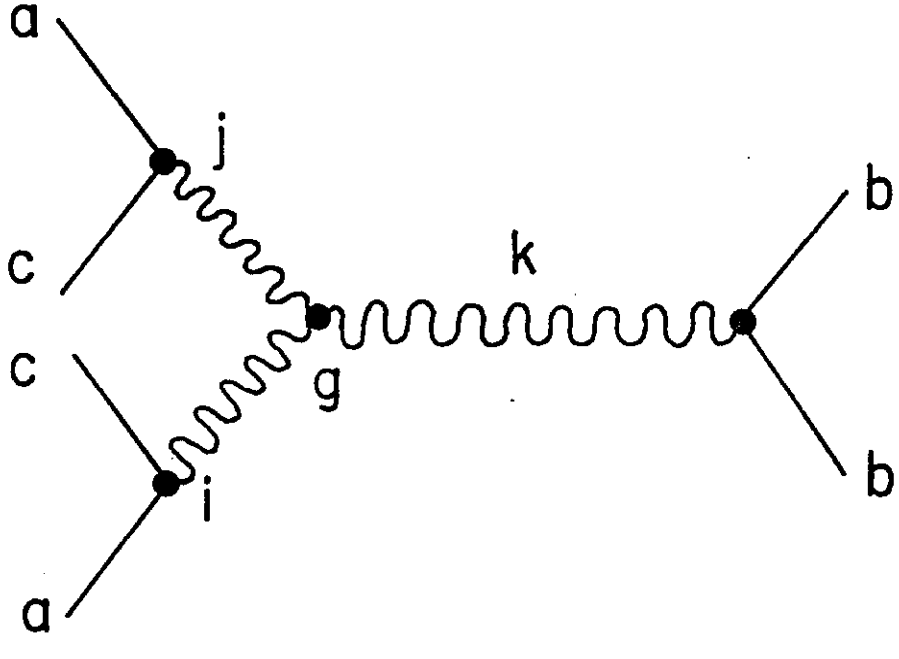

Fig. 8